



# Micromechanical properties of shear stiffening gel reinforced ethylene–vinyl acetate foam

Haowei Yang<sup>a,b,1</sup>, Huan Tu<sup>a,1</sup>, Zhe Yang<sup>a</sup>, Fan Tang<sup>a,b</sup>, Wenjian Cao<sup>a</sup>, Chenguang Huang<sup>a</sup>, Yacong Guo<sup>a,\*</sup>, Yanpeng Wei<sup>a,\*</sup>

<sup>a</sup> Key Laboratory for Mechanics in Fluid Solid Coupling Systems, Institute of Mechanics, Chinese Academy of Sciences, Beijing 100190, China

<sup>b</sup> School of Engineering Science, University of Chinese Academy of Sciences, Beijing 100049, China

## ARTICLE INFO

### Keywords:

Microstructure  
Shear stiffening gel  
Macroscopic mechanical properties  
Porous materials

## ABSTRACT

In previous study, a novel composite foam that possesses cushioning properties is developed by incorporating shear stiffening gel (SSG) into Ethylene-vinyl (EVA) foam. In this work, uniaxial compression is used to obtain the mechanical properties of the proposed material under static loading. The test results demonstrate the additive SSG could effectively enhance the energy absorption capacity. With the aid of in-situ Scanning Electron Microscope (SEM), two characteristics, the homogeneous microstructural morphology and phase separation between SSG and EVA, are found that played dominant roles in the improvement of cushioning properties.

## 1. Introduction

Shear stiffening gel (SSG) is a kind of polymer material with impact hardening characteristics. SSG behaves as a viscoelastic gel material under natural conditions, and its unique B-O bond allows its stiffness to rise rapidly when subjected to high velocity impacts [1–2].

Ethyl ethylene-acetate (EVA) foam is one of the widely used buffer materials for personal protection [3]. To develop novel foam materials with better anti-impact performance, incorporating modified agents into existing polymers has been an effective approach [4]. Due to its impact-hardening characteristic, SSG also has great potential for application in the development of cushioning materials [5–6].

Only limited studies of SSG modified foams have been reported and the reinforcement mechanism has not been distinctly elaborated. Thus, this work aims to investigate the mechanical behavior of EVA/SSG foams at both macroscopic and microscopic scale. Macroscopic mechanical properties, such as the quasi-static compressibility, are tested by the corresponding experimental methods. In addition, the authors investigate the effect of SSG on the micro-structure and micro-deformation behavior of matrix foam by scanning electron microscopy and in-situ compression.

## 2. Experimental

### 2.1. Preparation

Since the preparation of SSG and EVA/SSG has been elaborated in the authors' previous studies [7], the preparation processes of EVA/SSG foam and EVA foam are schematically presented in the Fig. 1(a). All the chemicals are supplied by Beijing CAS Mechanical Confidence Science and Technology Co., Ltd.

### 2.2. Characterization

Quasi-static compression tests are conducted using E1000 material testing machine (INSTRON Corporation) according to national standard GB/T 8168 2008. The geometry of specimens is 15 mm (diameter) × 5 mm (height). Specimens are compressed at three different strain rate levels (0.001, 0.01 and 0.1 s<sup>-1</sup>).

The in-situ SEM compression is conducted by using a quantitative SEM Picoindenter® system. A displacement-control mode is used at 1 μm/s. EVA and EVA/SSG foams are manufactured into 5 mm × 5 mm × 5 mm blocks for testing.

\* Corresponding authors.

E-mail addresses: [guoyacong@imech.ac.cn](mailto:guoyacong@imech.ac.cn) (Y. Guo), [weiyanyanpeng@imech.ac.cn](mailto:weiyanyanpeng@imech.ac.cn) (Y. Wei).

<sup>1</sup> Contributed equally in this work.

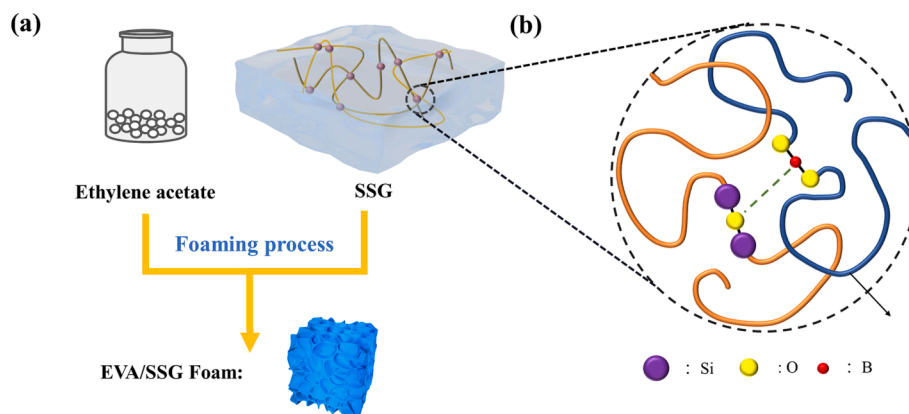


Fig. 1. (a) Preparation process of EVA/SSG foam. (b) Schematic diagram of SSG network cross-linked by boron-oxygen bonds.

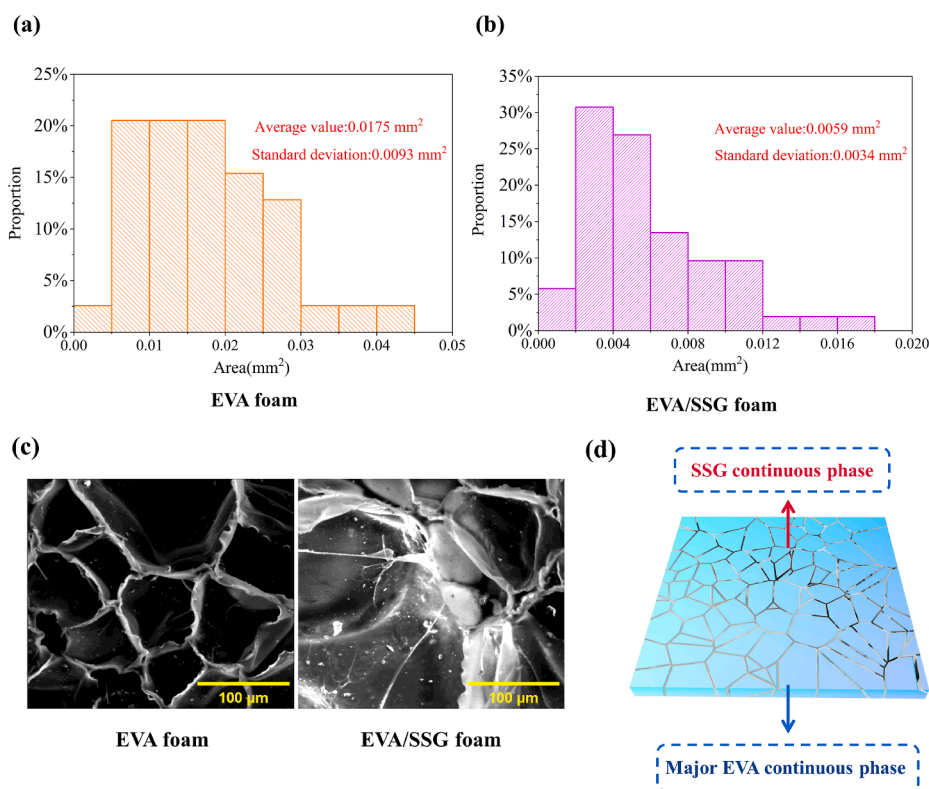


Fig. 2. (a) and (b) Cell area distribution of EVA foam and EVA/SSG foam. (c) SEM images of EVA foam and EVA/SSG foam. (d) Two-phase structure of SSG and EVA.

### 3. Results and discussion

#### 3.1. Cellular structure and surface morphology

As shown in Fig. 2(a) and (b), the average cell area of EVA/SSG foam is smaller than EVA foam, and the distribution of cell area is more uniform. The more inhomogeneous the area distribution, the larger the difference in the geometrical dimension of the cell. The individual cell can be thought of as a frame structure consisting of beams, thin walls, and rigid nodes. Considering the plastic buckling theory, the inhomogeneous cell structure of the EVA foam makes the critical load on the cells vary considerably. During compression, cells with low critical loads are the first to be crushed, creating a locally concentrated deformation region. The EVA/SSG foam has a smaller and more homogeneous cell structure. As a result, the potential failure in the localized regions can be suppressed to a certain extent and the bearing capacity to external loading is enhanced.

Fig. 2(d) shows the surface topography of the EVA/SSG foam. In contrast to the EVA foam (Fig. 2(c)), a large amount of filamentary SSG adhering to the cell wall is observed in the EVA/SSG foam. The microscopical image Fig. 2(c) indicates that EVA/SSG foam possesses a typical two-phase separation structure, which is conducive to reserve the material properties of SSG and EVA [8].

#### 3.2. Quasi-static compression experiments

Fig. 3(a) displays the stress–strain curves of EVA foam and EVA/SSG foam under different rates of compression. As clearly shown in the figure, the stress–strain curves of EVA/SSG foams can be divided into three regions. In region I, foams behave as linear elastic material. In region II, plastic deformation is observed with long stress plateau, which is caused by plastic deformation of cellular structures [9]. Moreover, plastic deformations can absorb large amounts of energy. In region III, foams begin to enter the densification stage and the stiffness rises

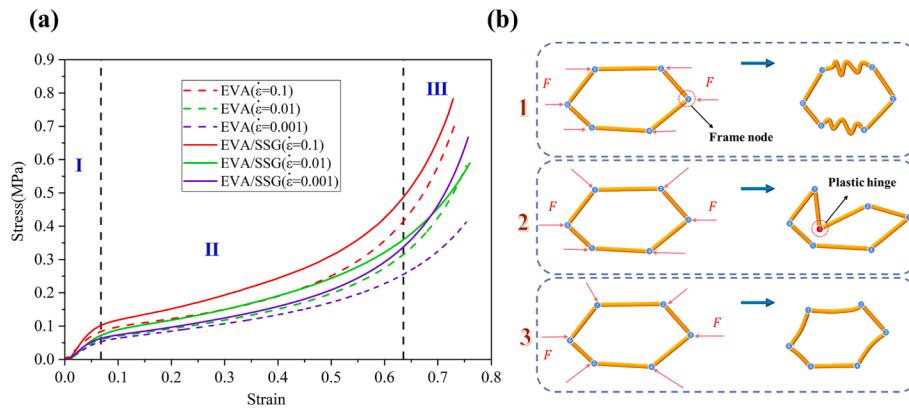


**Fig. 3.** (a) Stress–strain curve of compression test at 0.001, 0.01 and 0.1 s<sup>-1</sup> strain rate. (b) Three basic deformation modes of single cell structure, 1: plastic crushing deformation, 2: plastic bending deformation, 3: elastic bending deformation.

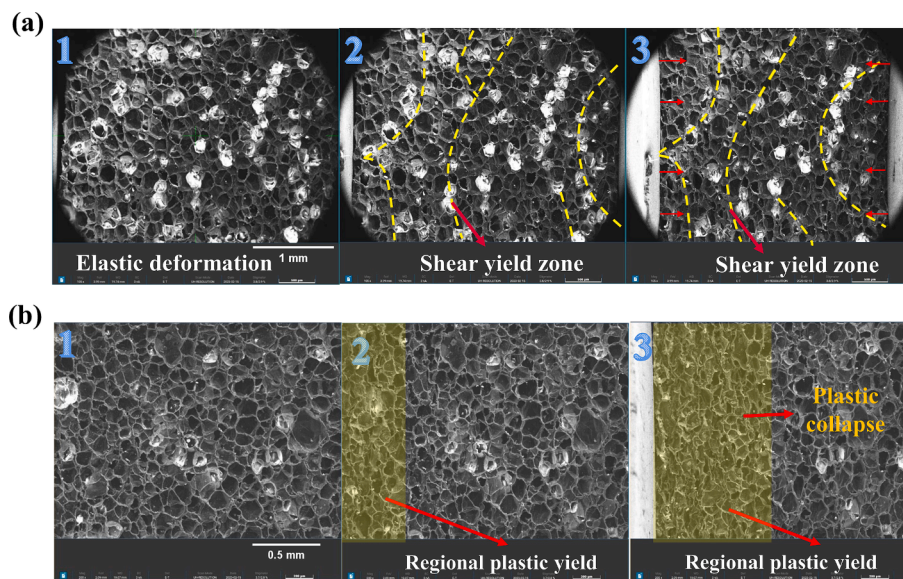


**Fig. 4.** In-situ SEM micrographs of EVA foam and EVA/SSG foam (a) and (b), reflecting 1: the elastic region, 2: yield point, 3: plastic crushing.

sharply.

Compared to EVA foam, EVA/SSG foam has higher yield stress and plastic plateau stress. This phenomenon indicates that the SSG can assist the EVA to resist external loading during compression and the EVA/SSG foam has a better energy absorption capacity during compression.

### 3.3. In-situ SEM compression

Fig. 4(a) and (b) are a set of microstructural images of EVA foam and EVA/SSG foam during in-situ compression. In the elastic region, EVA foam (Fig. 4(a-1)) and EVA/SSG foam (Fig. 4(b-1)) undergo overall elastic deformation, where elastic bending of cell walls is observed (Fig. 3(b-3)). At yield point of EVA foam (Fig. 4(a-2)), plastic deformation occurs first in cells with lower yield strength, and these cells are connected to each other to form an inclined plastic yield band. EVA/SSG (Fig. 4(b-2)) foam began to exhibit regional plastic deformation. With the continuing compression, cells of EVA foam and EVA/SSG foam begin to enter the plastic deformation stage as the patterns shown in Fig. 4(a-3) and Fig. 4(b-3), and the cells with higher strength in EVA foam begin to undergo gradual plastic deformation. Unlike the EVA foams, the EVA/SSG foams have a distinct feature of region yielding, which is attributed to the non-uniform distribution of SSG in the EVA/SSG foams. SSG also influences the deformation mode of EVA foam. As shown in Fig. 4, the

cells of EVA foam exhibit plastic bending mode (Fig. 3(b-2)), where its cell edges and cell walls undergo plastic bending deformation and form plastic hinges. For EVA/SSG foams, cell edges and cell walls undergo plastic collapse (Fig. 3(b-1)).

The crushed cells of the EVA foam in the concentrated region do not favor the transfer of impact energy to the surrounding region. In the composite foam, SSG significantly increases the connectivity between cell structures, which contributes to shock wave propagation and impact energy consumption. At the same time, SSG effectively affects the plastic deformation mode of the cell and improv its energy absorption capacity.

## 4. Conclusions

Based on the test results, it is found that the addition of SSG significantly improves the yield strength and plastic platform stress, and thus the EVA/SSG foam has better energy absorption. In addition, SEM images demonstrate a uniform distribution of cells in the EVA/SSG foam and filamentous SSG attachment to the cell walls.

Furthermore, the experimental results of in -situ compression test shows that SSG affects the microscopic deformation behavior of EVA foams in two ways. First, SSG changes the cell from plastic bending mode to plastic crushing mode, which improves the energy absorption efficiency of the cell. Second, SSG modifies the plastic deformation

evolution of the EVA foam, such that EVA foam changes from localized concentrated deformation to regional global deformation.

#### CRediT authorship contribution statement

**Haowei Yang:** Methodology, Writing – original draft. **Huan Tu:** Conceptualization, Investigation, Supervision. **Zhe Yang:** Methodology, Validation. **Fan Tang:** Resources. **Wenjian Cao:** Software, Investigation. **Chenguang Huang:** Methodology, Conceptualization. **Yacong Guo:** Resources, Funding acquisition, Writing – review & editing. **Yanpeng Wei:** Resources, Funding acquisition, Writing – review & editing.

#### Declaration of Competing Interest

The authors declare that they have no known competing financial interests or personal relationships that could have appeared to influence the work reported in this paper.

#### Data availability

The data that has been used is confidential.

#### Acknowledgments

This work is supported by the National Natural Science Foundation

of China (Grant No.12072356 and No.12232020) and the Science and Technology on Transient Impact Laboratory (Grant No. 6142606221105).

#### References

- [1] Weifeng Jiang, et al., Strain rate-induced phase transitions in an impact-hardening polymer composite, *Appl. Phys. Lett.* 104 (12) (2014), <https://doi.org/10.1063/1.4870044>.
- [2] Chunyu Zhao, et al., Shear stiffening gels for intelligent anti-impact applications, *Cell Rep. Phys. Sci.* 1 (12) (2020), <https://doi.org/10.1016/j.xcrp.2020.100266>.
- [3] C. Lam, J.S.H. Kwan, Y. Su, et al., Performance of ethylene-vinyl acetate foam as cushioning material for rigid debris-resisting barriers, *Landslides* 15 (2018) 1779–1786, <https://doi.org/10.1007/s10346-018-0987-z>.
- [4] Gao Sheng, et al., Synthesis of borosiloxane/polybenzoxazine hybrids as highly efficient and environmentally friendly flame retardant materials, *J Polym. Sci., Part A: Polym. Chem.* 55 (2017) 2390–2396, <https://doi.org/10.1002/pola.28628>.
- [5] Wang Sheng, et al., Stretchable polyurethane sponge scaffold strengthened shear stiffening polymer and its enhanced safeguarding performance, *ACS Appl. Mater. Interfaces* 8 (7) (2016) 4946–4954, <https://doi.org/10.1021/acsami.5b12083>.
- [6] X. Liu, C. Qian, et al., Energy absorption and low-velocity impact response of shear thickening gel reinforced polyurethane foam, *Smart Mater. Struct.* 29 (4) (2020), <https://doi.org/10.1088/1361-665X/ab73e2>.
- [7] Tang Fan, et al., Protective performance and dynamic behavior of composite body armor with shear stiffening gel as buffer material under ballistic impact, *Compos. Sci. Technol.* (2020) 218, <https://doi.org/10.1016/j.compscitech.2021.109190>.
- [8] Je Kyum Lee, et al., Evolution of polymer blend morphology during compounding in a twin-screw extruder, *Polymer* 41 (5) (2000) 1799–1815, [https://doi.org/10.1016/S0032-3861\(99\)00325-0](https://doi.org/10.1016/S0032-3861(99)00325-0).
- [9] Yu Xuan, et al., Numerical simulation of static mechanical properties of PMMA microcellular foams, *Compos. Sci. Technol.* 192 (2020), <https://doi.org/10.1016/j.compscitech.2020.108110>.